MSc. Data Science & AI

Class: Biomedical Signal Processing

Blind source separation

Professor: Vicente Zarzoso

Student: Aglind Reka

Report

Contents

1 Synthetic signals **1**

1.1 Repeat Exercises 5–7 of the course after reducing the desired signal power contribution to the first sensor to 0.01. Conclude. 1

1.2 Effects of desired signal leakage into the reference signals. Retrieve the observed signals from experiment 2.1-2, where the reference signals were contaminated by components of the signal of interest. Repeat Exercises 5–7 of the course with these observations. Conclude. 5

2 Fetal ECG extraction **7**

3 Atrial activity extraction — single patient **11**

4 Atrial activity extraction — full database **13**

1. Synthetic signals

1.1 Repeat Exercises 5–7 of the course after reducing the desired signal power contribution to the first sensor to 0.01. Conclude.

Table 1: Orthogonality Check and Signal Quality Evaluation

Evaluation Metric	**Value**
Orthogonality Check	Correctly controlled
Contribution of Desired Signal to Primary Signal (First Sensor)	0.92507
Power of Desired Signal	0.5
Power of Observed Signal (Primary Input)	5.405
Power of Estimated Signal	1
Power of Error Signal	1.1311
Signal-to-Interference Ratio (SIR) of Estimated Signal	-6.9897 dB
SIR Improvement brought by BSS-PCA	3.0103 dB

As shown in Table 1:
Orthogonality Check: Confirms successful control of orthogonality, indicating effective separation between the desired signal and interference.

Contribution of Desired Signal to Primary Signal (First Sensor): The desired signal contributes 0.92507 to the primary signal in the first sensor post-separation, indicating significant retention of the desired signal.

Power of Desired Signal: The original power of the desired signal is 0.5.

Power of Observed Signal (Primary Input): Post-separation, the observed signal's power is 5.405, indicating signal amplification compared to the original desired signal.

Power of Estimated Signal: The estimated signal's power post-separation is 1.

Power of Error Signal: A residual interference or noise results in an error signal power of 1.1311.

Signal-to-Interference Ratio (SIR) of Estimated Signal: The SIR of the estimated signal is -6.9897 dB, indicating a stronger presence of interference compared to the desired signal.

SIR Improvement brought by BSS-PCA: BSS-PCA enhances SIR by 3.0103 dB, demonstrating improved signal quality through interference reduction.

In Figure 1, it is evident that the amplitude of the waves in PCA source 1 is notably larger compared to those in PCA source 2, which are relatively less pronounced and discernible. Both sources exhibit frequent oscillations over time, indicating dynamic patterns. However, PCA source 2 displays less frequent oscillations compared

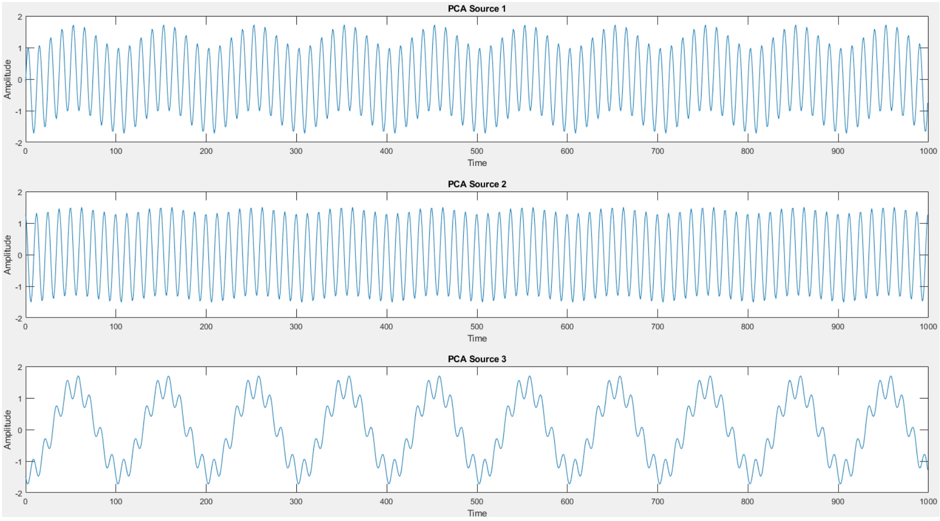

Figure 1: Ploting: PCA Sources

to PCA source 1, suggesting potential variations in underlying dynamics or signal characteristics.

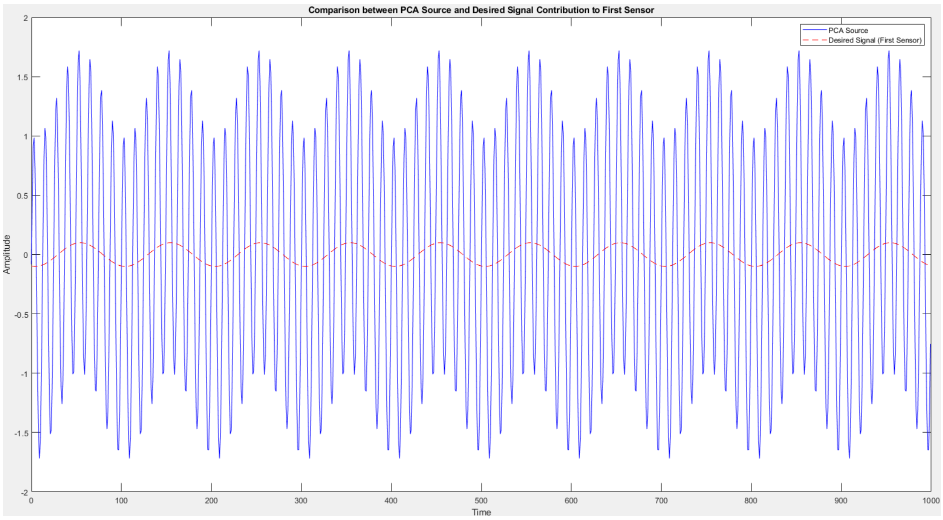

Figure 2: Ploting: Comparison between PCA Source and Desired Signal Contribution to First Sensor

As we can observe in Figure 2, the PCA source exhibits larger fluctuations compared to the desired signal contribution, suggesting the presence of additional variability or noise captured by the PCA. While the desired signal maintains regular and standardized waveforms, indicating signal fidelity, the PCA source may contain unwanted noise or interference.

In Figure 3, we notice a distinction between the desired signal and the estimated signals. The desired signal exhibits regular waveform patterns with longer intervals between peaks, suggesting a stable and predictable signal behavior over time. In contrast, the estimated signals display more frequent and varied waveform patterns, often with higher amplitudes and closer peaks. This difference indicates that the estimated

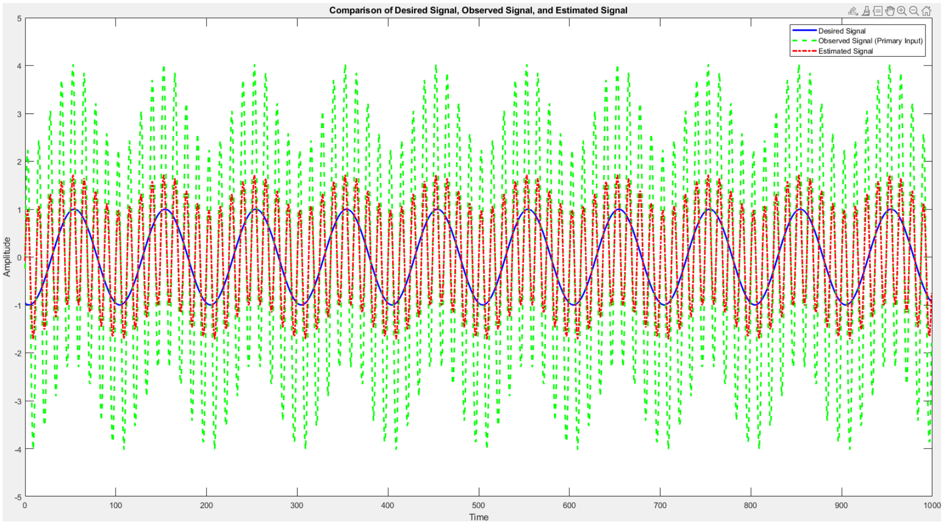

Figure 3: Ploting: Comparison of Desired Signal, Observed Signal, and Estimated Signal

signals may contain additional fluctuations or noise compared to the desired signal, emphasizing the importance of signal fidelity assessment in separation algorithms.

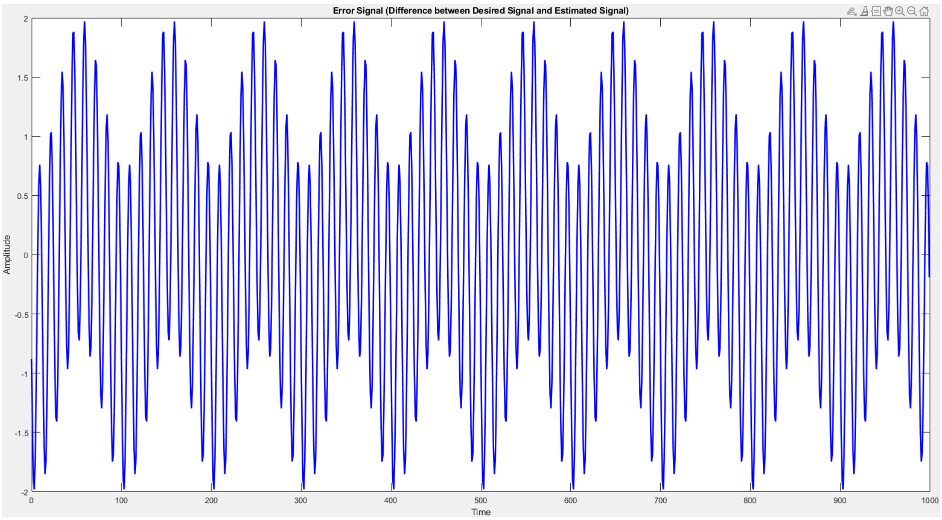

Figure 4: Ploting: Error Signal (Difference between Desired Signal and Estimated Signal)

In Figure 4, the error signals exhibit waveform amplitudes ranging from -2 to 2, indicating a moderate fluctuation around the zero baseline. The waveform patterns appear regular in time, suggesting consistent fluctuations throughout the observation period.

In Figure 5, the frequency spectrum comparison illustrates distinct peaks in the lower frequency range for all three signals, indicating significant spectral components within this range. These peaks likely represent fundamental frequency components of the signals, reflecting their dominant spectral content.

Furthermore, a secondary peak is observed around 40 Hz in both the desired and

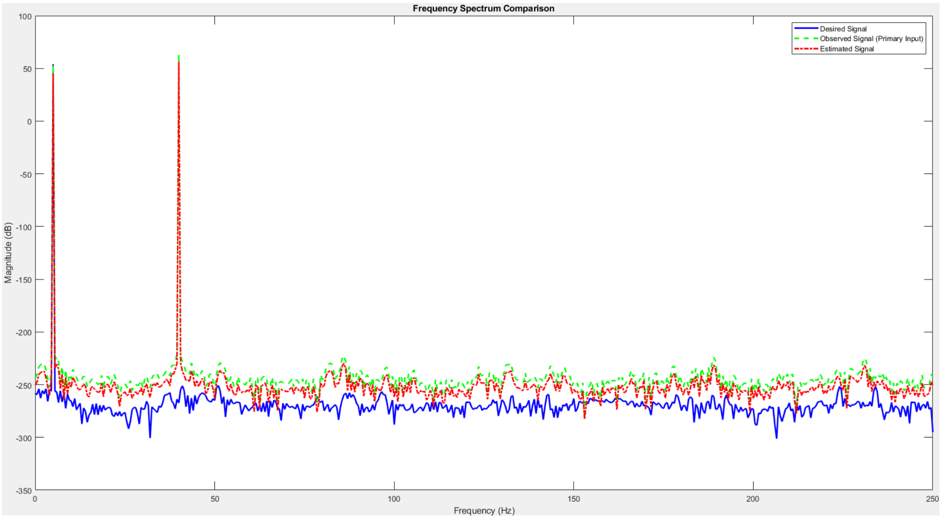

Figure 5: Ploting: Frequency Spectrum Comparison

observed signals. This secondary peak can suggest the presence of specific frequency components or noise sources contributing to the signals within this frequency band.

Moreover, the magnitude of the spectral components remains relatively stable, ranging between approximately -300 and -220 dB. This consistent magnitude suggests that the signals maintain their spectral characteristics across the frequency spectrum, with no significant variations in energy levels. However, the negative dB values indicate that the spectral components are relatively low in magnitude, which could be attributed to the presence of noise or interference in the signals.

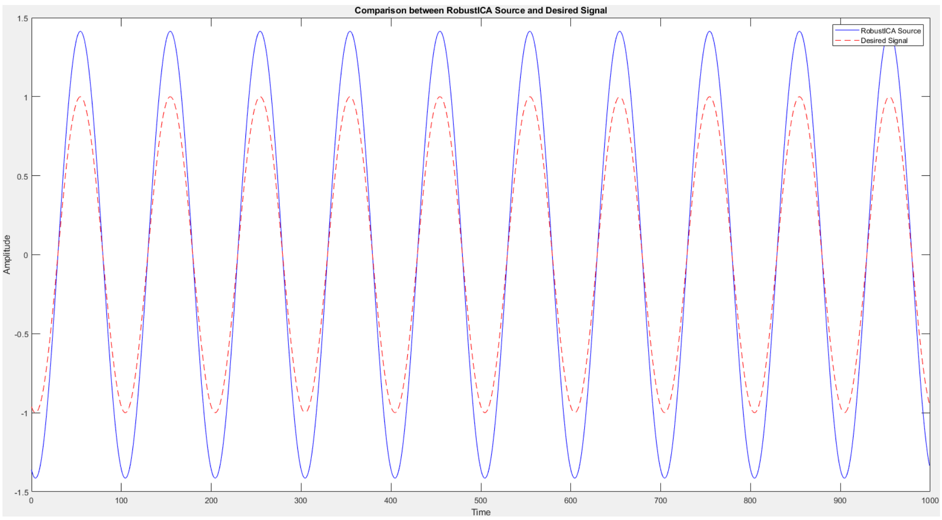

Figure 6: Ploting: Comparison between RobustICA Source and Desired Signal

In Figure 6, it's apparent that the robustICA source closely resembles the desired signal, exhibiting similar waveforms. This similarity suggests that the robustICA algorithm has effectively captured the essential characteristics of the desired signal during the separation process.

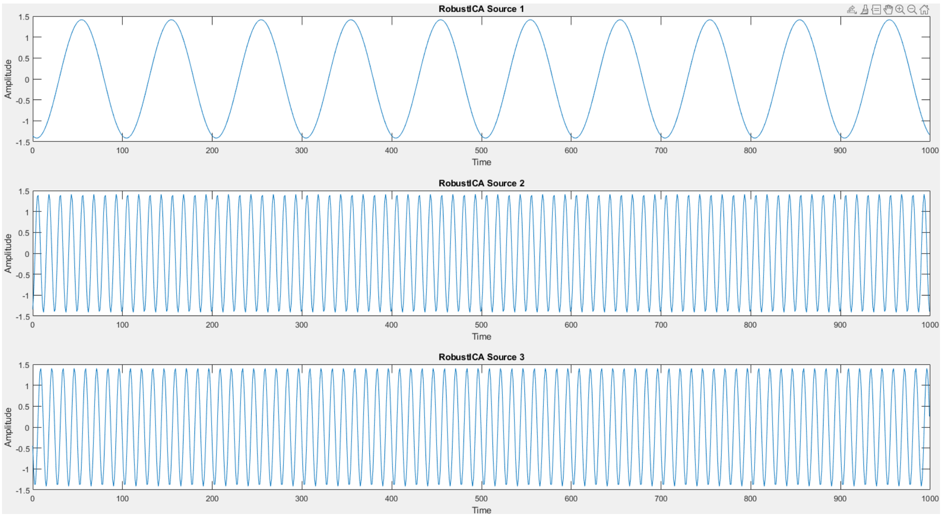

Figure 7: Ploting: RobustICA Sources

1.2 Effects of desired signal leakage into the reference signals. Retrieve the observed signals from experiment 2.1-2, where the reference signals were contaminated by components of the signal of interest. Repeat Exercises 5–7 of the course with these observations. Conclude.

Table 2: Orthogonality Check and Signal Quality Evaluation (Contaminated by components of the signal of interest)

Evaluation Metric	**Value**
Orthogonality Check	Correctly controlled
Contribution of Desired Signal to Primary Signal (First Sensor)	0.92507
Power of Desired Signal	0.5
Power of Observed Signal (Primary Input)	5.405
Power of Estimated Signal	1
Power of Error Signal	1.858
Signal-to-Interference Ratio (SIR) of Estimated Signal	-6.9897 dB
SIR Improvement brought by BSS-PCA	3.0103 dB

In Table 2, the only notable difference observed under the "Contaminated by components of the signal of interest" criterion is a 1.858-unit increase in the Power of Error Signal. This signifies that when the signal of interest is tainted by its own components, the resultant error signal exhibits a higher power level by 1.858 units. This suggests that the interference or noise originating from the signal itself contributes to an elevated power level in the error signal, contrasting with the scenario where the signal remains uncontaminated by its own components.

Following the contamination by components of the signal of interest, the observed discrepancy in peak patterns among the signals in Figure 10 suggests a significant

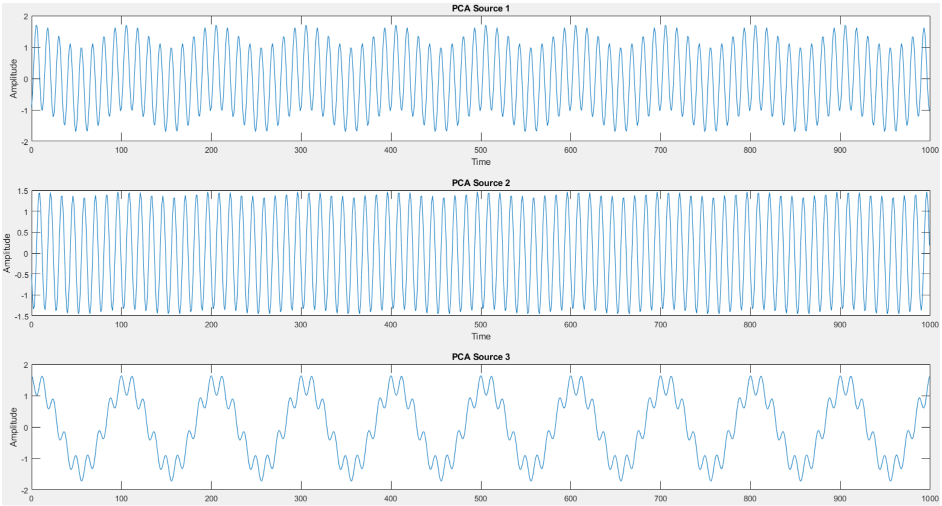

Figure 8: Ploting: PCA Sources (Contaminated by components of the signal of interest)

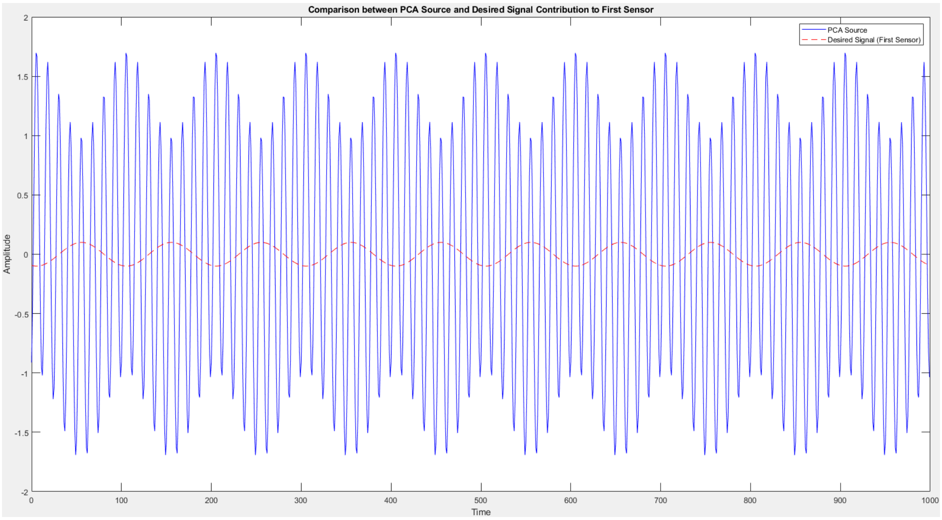

Figure 9: Ploting: Comparison between PCA Source and Desired Signal Contribution to First Sensor (Contaminated by components of the signal of interest)

alteration in signal characteristics. This discrepancy indicates that the contamination has introduced variations in the frequency components or dynamics of the signals, leading to inconsistencies in their peak patterns. Consequently, we can infer that the contamination has adversely affected the quality and integrity of the signals, resulting in notable changes in their behavior post-separation.

As evident from Figure 14, the robustICA source exhibits a distinct deviation from the desired signal, showcasing a considerable divergence. The contamination by components of the signal of interest appears to have exerted a more pronounced influence in this instance, notably altering the characteristics of the robustICA source compared to the desired signal.

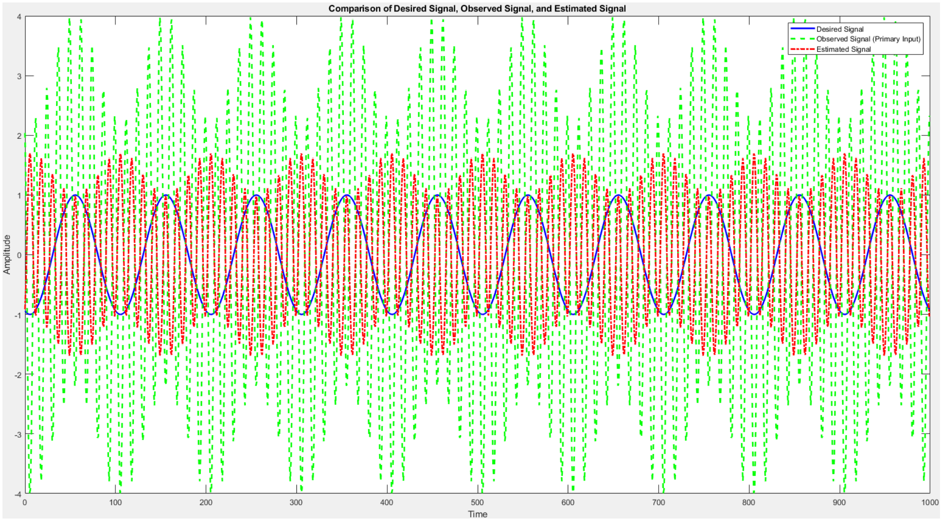

Figure 10: Ploting: Comparison of Desired Signal, Observed Signal, and Estimated Signal (Contaminated by components of the signal of interest)

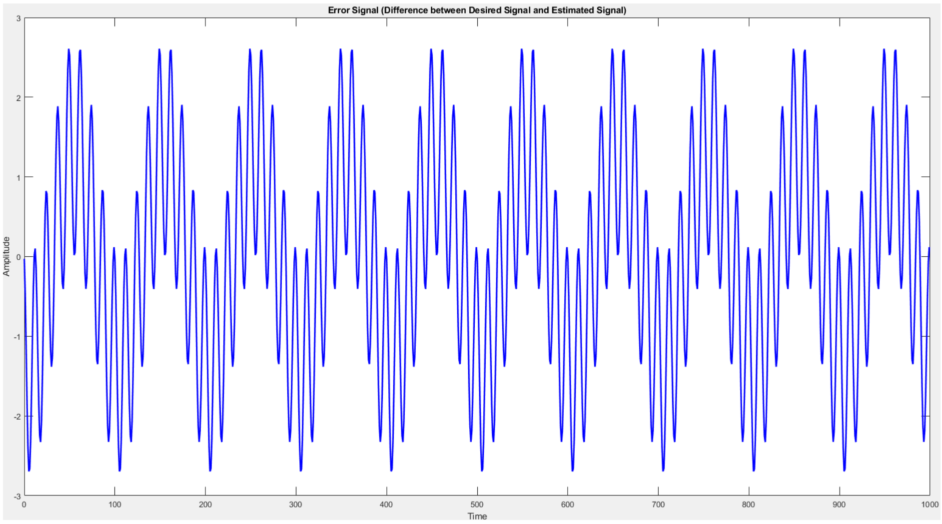

Figure 11: Ploting: Error Signal (Difference between Desired Signal and Estimated Signal) (Contaminated by components of the signal of interest)

2. Fetal ECG extraction

In Figure 15, we can examine the eight plotted sources to discern patterns indicative of fetal ECG activity. Upon closer scrutiny, sources 4 and 8 stand out for their notable irregularities in waveform compared to the others. These irregularities are characterized by sudden amplitude and frequency fluctuations, often associated with fetal cardiac activity. The variability in fetal heart rhythm, influenced by factors such as movement and developmental stage, can manifest as irregular patterns.

Turning attention to Figure 16, our analysis focuses on sources 6, 7, and 8, where we again detect pronounced irregularities in waveform patterns. Notably, these irregularities are more conspicuous in the latter sources, hinting at a higher likelihood

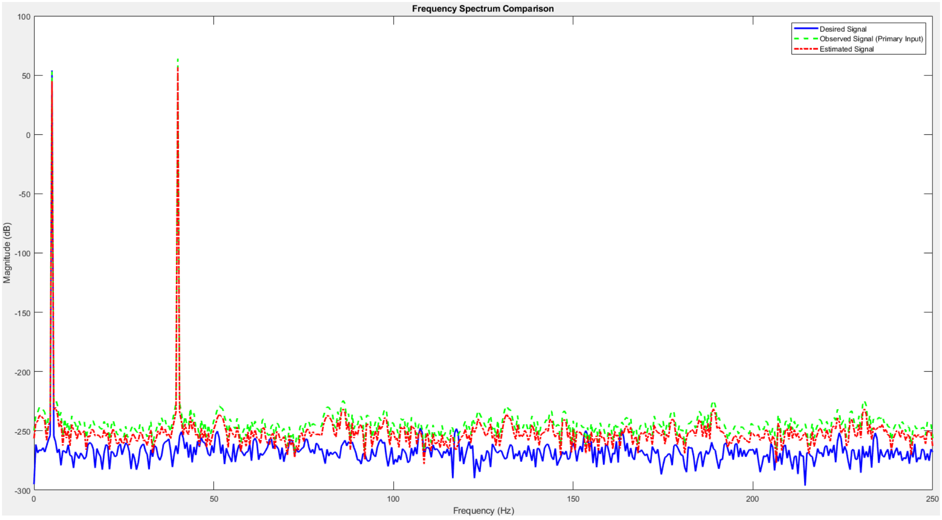

Figure 12: Ploting: Frequency Spectrum Comparison (Contaminated by components of the signal of interest)

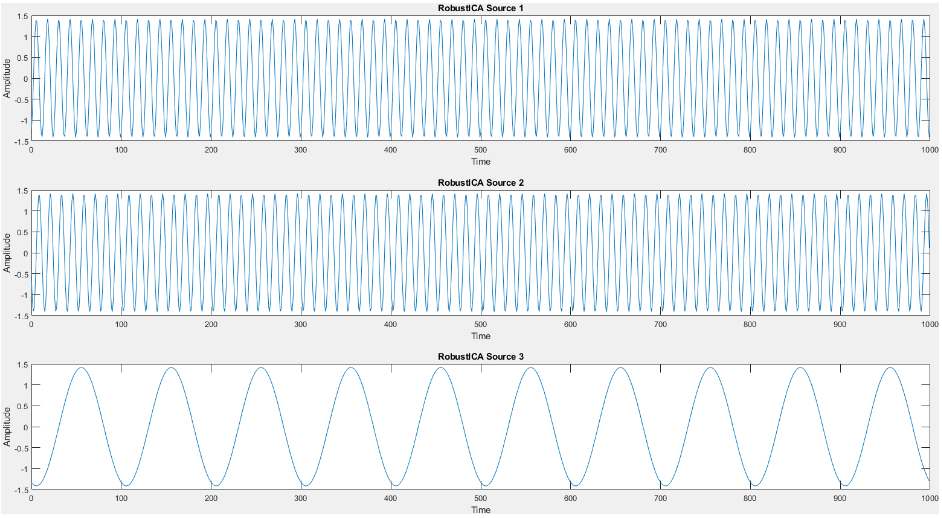

Figure 13: Ploting: RobustICA Sources (Contaminated by components of the signal of interest)

of fetal cardiac activity.

Comparing the abdominal signals with the estimated FECG contributions reveals distinct waveform characteristics as we can observe in 17, 18:

Abdominal Signals:

- Most abdominal signals exhibit regular waveforms, with only minor irregularities observed in the 4th signal.
- Overall, the abdominal signals maintain consistent waveform patterns with minimal variation.

Estimated FECG Contributions:

- PCA Estimated FECG: Demonstrates relatively regular waveform patterns, al-

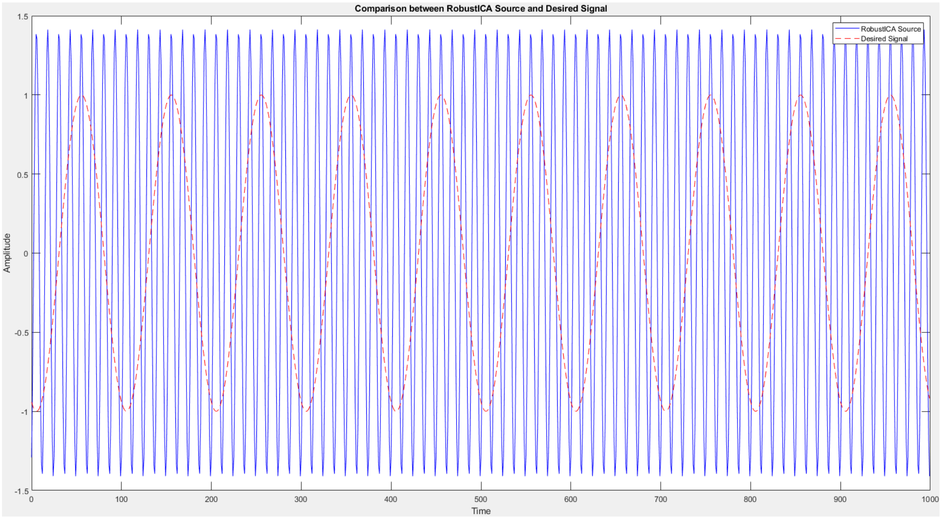

Figure 14: Ploting: Comparison between RobustICA Source and Desired Signal (Contaminated by components of the signal of interest)

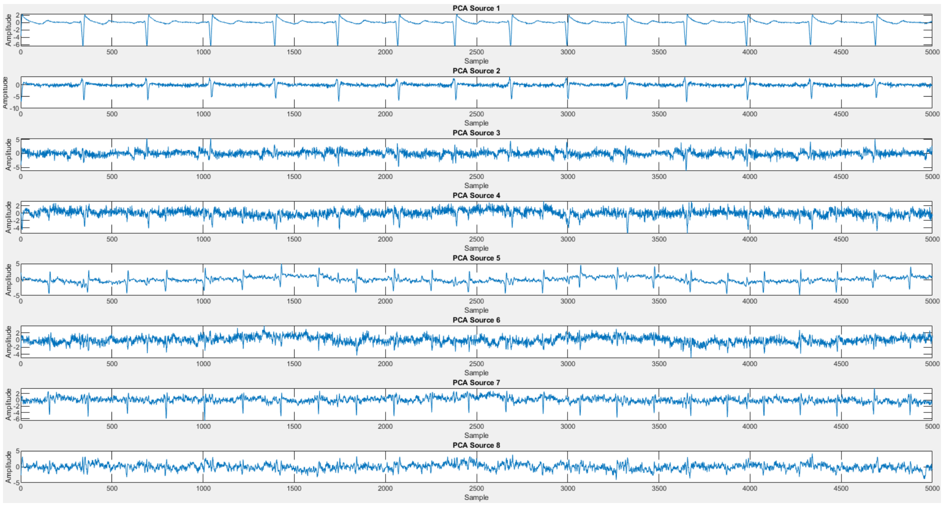

Figure 15: Ploting: PCA Sources

beit with some variability evident.

- ICA Estimated FECG: Displays higher regularity in time compared to PCA, indicating smoother waveform patterns.

Comparison:

- Abdominal signals present a mixture of regular and slightly irregular waveforms, with minimal deviations across signals.
- In contrast, both PCA and ICA estimated FECG contributions exhibit greater regularity, particularly noticeable in ICA.
- While PCA shows some irregularity akin to abdominal signals, ICA captures smoother and more consistent waveform patterns.

This comparison underscores the differences in waveform characteristics, empha-

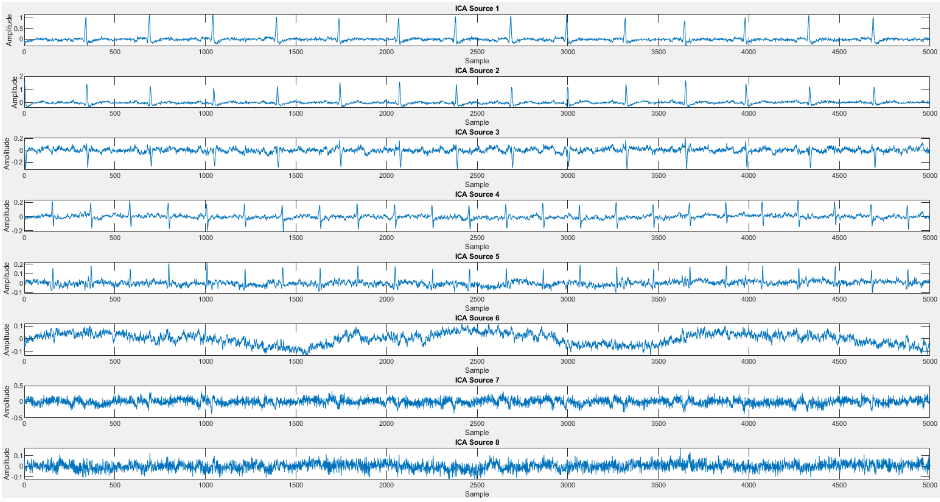

Figure 16: Ploting: Comparison between PCA Source and Desired Signal Contribution to First Sensor

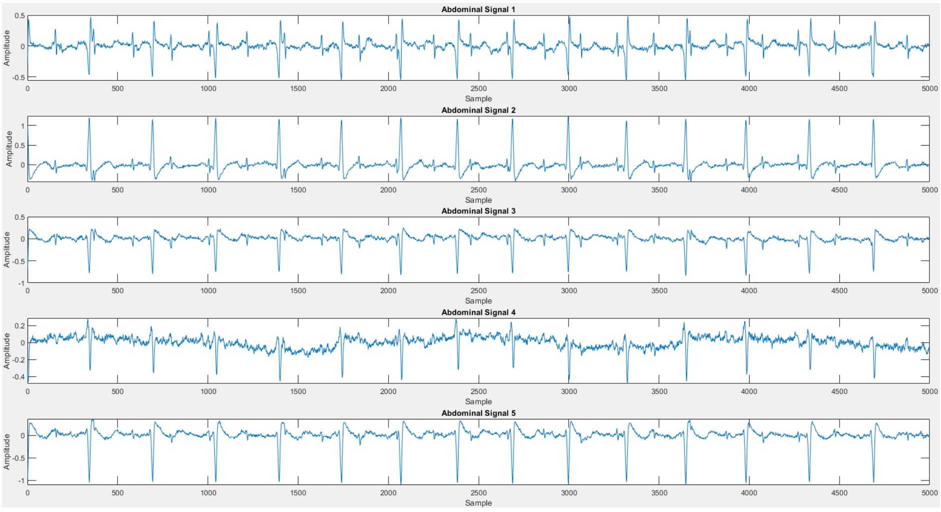

Figure 17: Ploting: Frequency Spectrum Comparison

sizing the ability of ICA to yield more coherent FECG estimates compared to PCA, which aligns more closely with the regularity observed in abdominal signals.

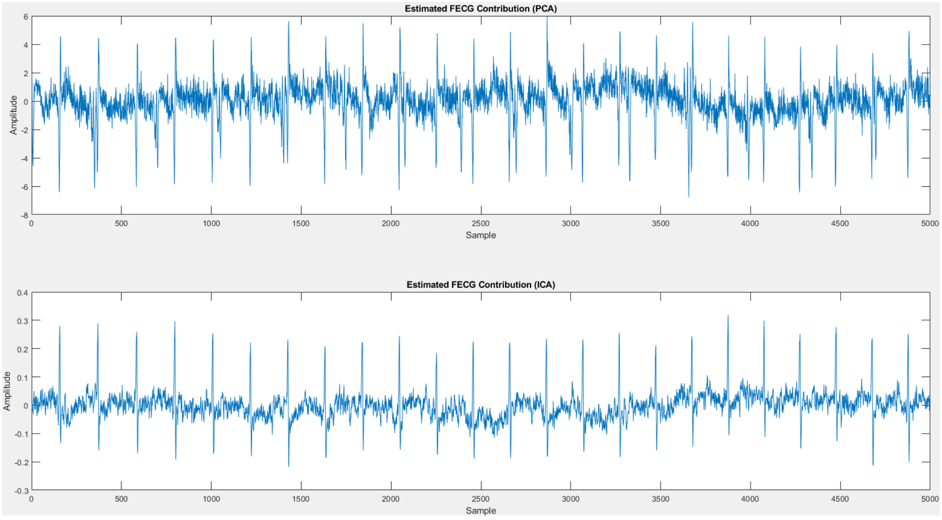

Figure 18: Ploting: Comparison between RobustICA Source and Desired Signal

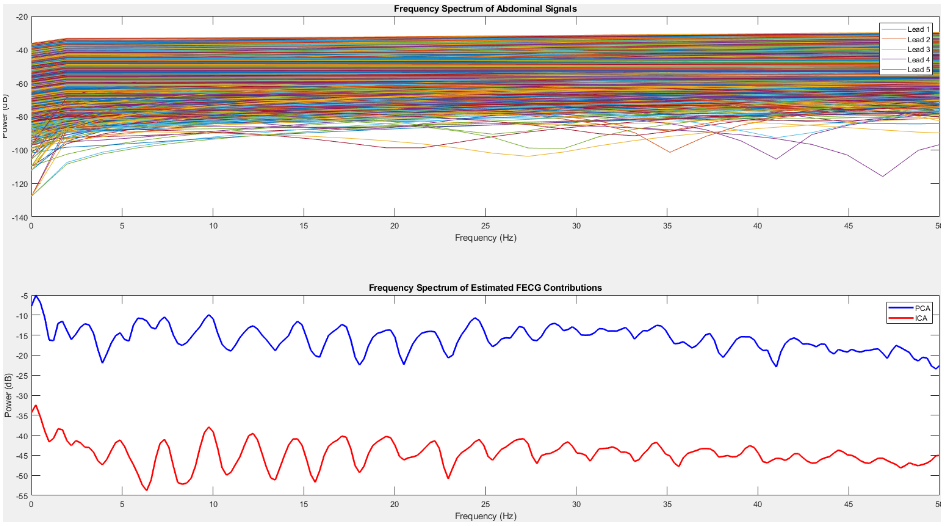

Figure 19: Ploting: RobustICA Sources

3. Atrial activity extraction — single patient

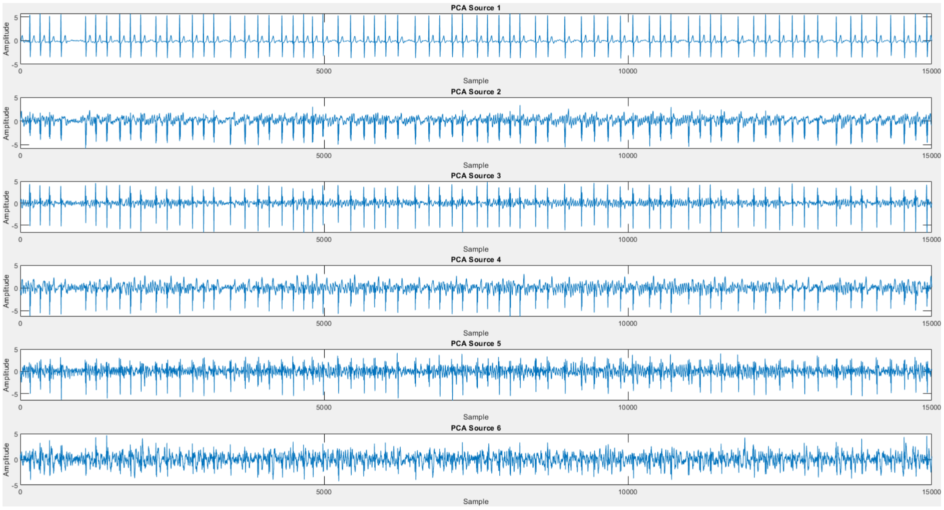

Figure 20: Ploting: RobustICA Sources

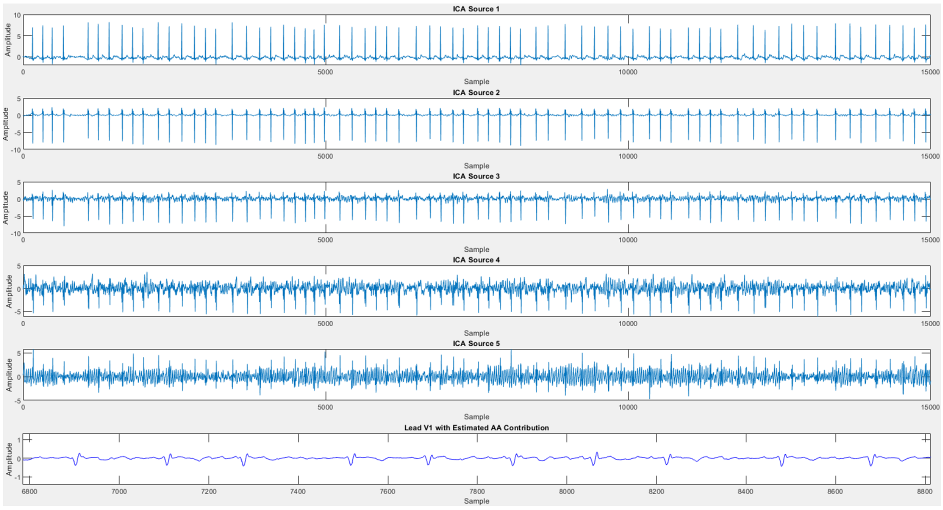

Figure 21: Ploting: RobustICA Sources

In Figure 20, irregularities are noticeable in the waveforms of PCA sources 2, 4, 5, and 6, with source 4 exhibiting slight irregularities. These deviations raise doubts regarding their association with atrial activity (AA). Conversely, in Figure 21, irregular waveform patterns are observed in sources 4 and 5, further suggesting potential involvement in atrial activity. In the last sources, we can observe signals on lead V1 and superimposed the estimated AA contribution.

Referring to Figure 22, it's evident that the two observed contributions closely resemble each other, displaying similar waveform characteristics. However, they appear to be distinctly distant from the signal observed in Lead 1.

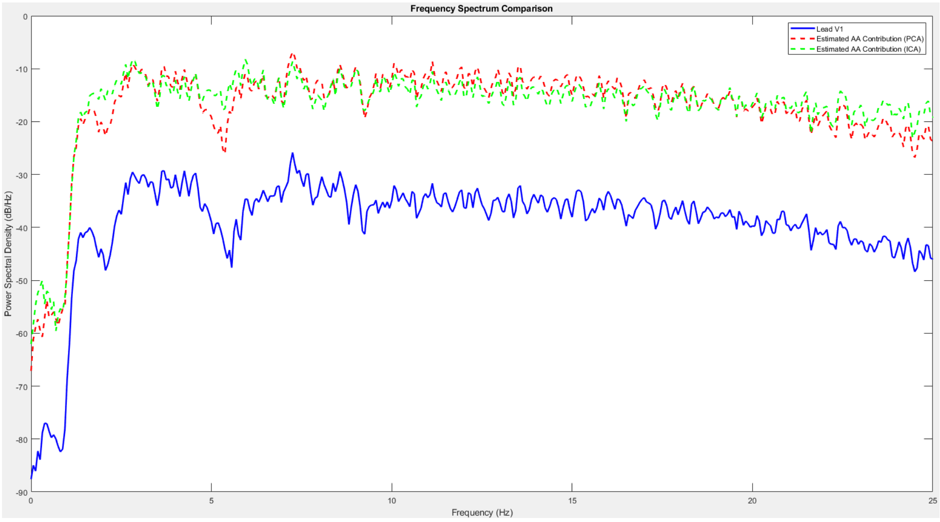

Figure 22: Ploting: RobustICA Sources

Table 3: Performance Metrics

Metric	Value
Average Accuracy	0.4641
Average Precision	0.4965
Average Recall	0.6286
Average F1-score	0.5186
Average ROC AUC	0.4990

4. Atrial activity extraction — full database

Average Accuracy: 46.41**Average Precision**: 49.65**Average Recall**: 62.86**Average F1-score**: 51.86**Average ROC AUC**: 49.90These metrics provide a concise overview of the model's performance in predicting AF recurrence, indicating moderate accuracy, precision, recall, and F1-score, with the ROC AUC slightly better than random chance.

In Figure 23, the box plot visualization of the DF (Dominant Frequency) parameter reveals interesting insights across the different methods:

Similar Distribution: Across PCA, ICA, MRANC, and STC methods, the distribution of DF appears relatively similar, with median values and interquartile ranges showing comparable trends. This suggests consistency in estimating the dominant frequency of the atrial sources across these methods.

STC Outliers: Notably, in the case of STC, approximately 50% of the data is concentrated within the range of 8 to 9 Hz. This concentrated distribution suggests a specific clustering of DF values for STC, potentially indicative of distinct characteristics in the estimated atrial sources compared to other methods.

PCA Outliers: PCA exhibits a higher prevalence of outliers compared to the

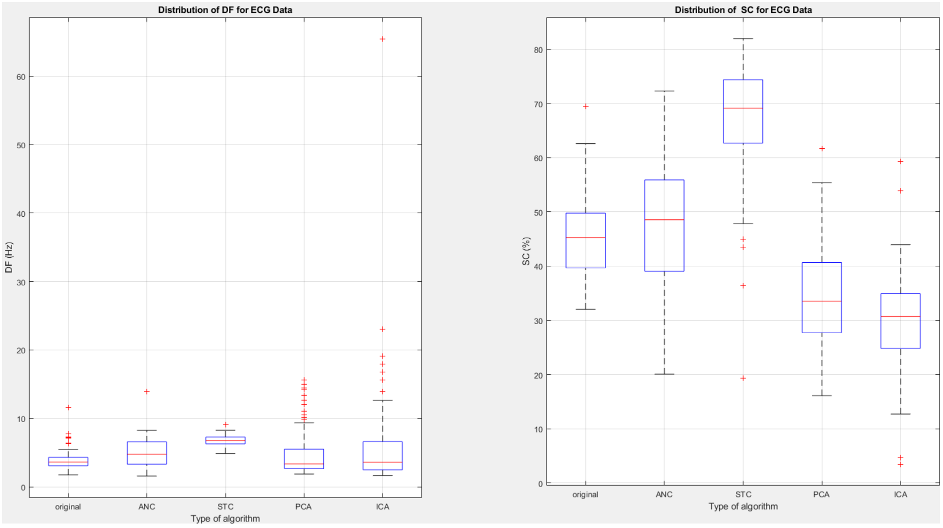

Figure 23: Ploting: Box Plots

other methods. These outliers may represent instances where PCA estimation deviates from the expected distribution of DF values, possibly due to inherent limitations in the PCA approach.

Instead, for the SC parameter, I observe more diversity between the different methods. In this case, STC exhibits higher values in its distribution compared to the other methods. This indicates a potential difference in the coherence or consistency of the estimated atrial sources by STC, leading to higher SC values. The variations in SC across methods suggest distinct approaches and performance characteristics in estimating the spectral coherence of atrial activity.